eLIFE
elifesciences.org

Figures and figure supplements

Extensive site-directed mutagenesis reveals interconnected functional units in the alkaline phosphatase active site

Fanny Sunden, et al.

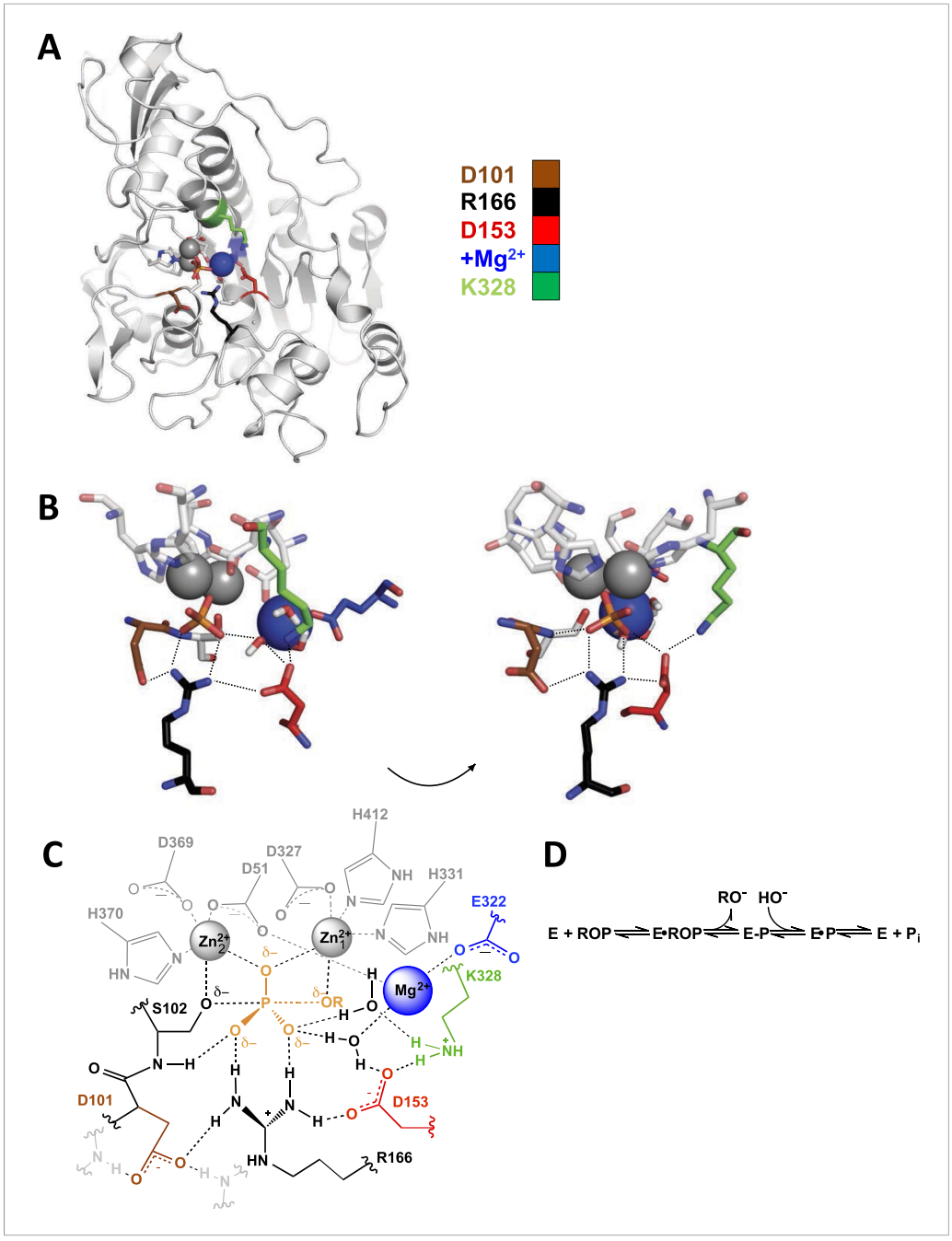

Figure 1. Alkaline phosphatase (AP) structure and active site. (**A**) The three-dimensional structure of AP with bound P_i (PDB 3TG0). Active site residues are depicted as follows: D101, brown; R166, black; D153, red; K328, green; E322 and Mg^{2+} ion, blue. (**B**) A close-up of AP active site from two angles. Dashes represent putative hydrogen bonds. Residues colored as in part (**A**). (**C**) Schematic of AP active site interactions represented with the phosphoryl transfer transition state. Residues colored as in part (**A**). (**D**) Reaction scheme for phosphomonoester hydrolysis by AP, where ROP represents a phosphate monoester dianion substrate, and E-P represents the covalent seryl-phosphate intermediate (***Coleman, 1992***).

DOI: 10.7554/eLife.06181.003

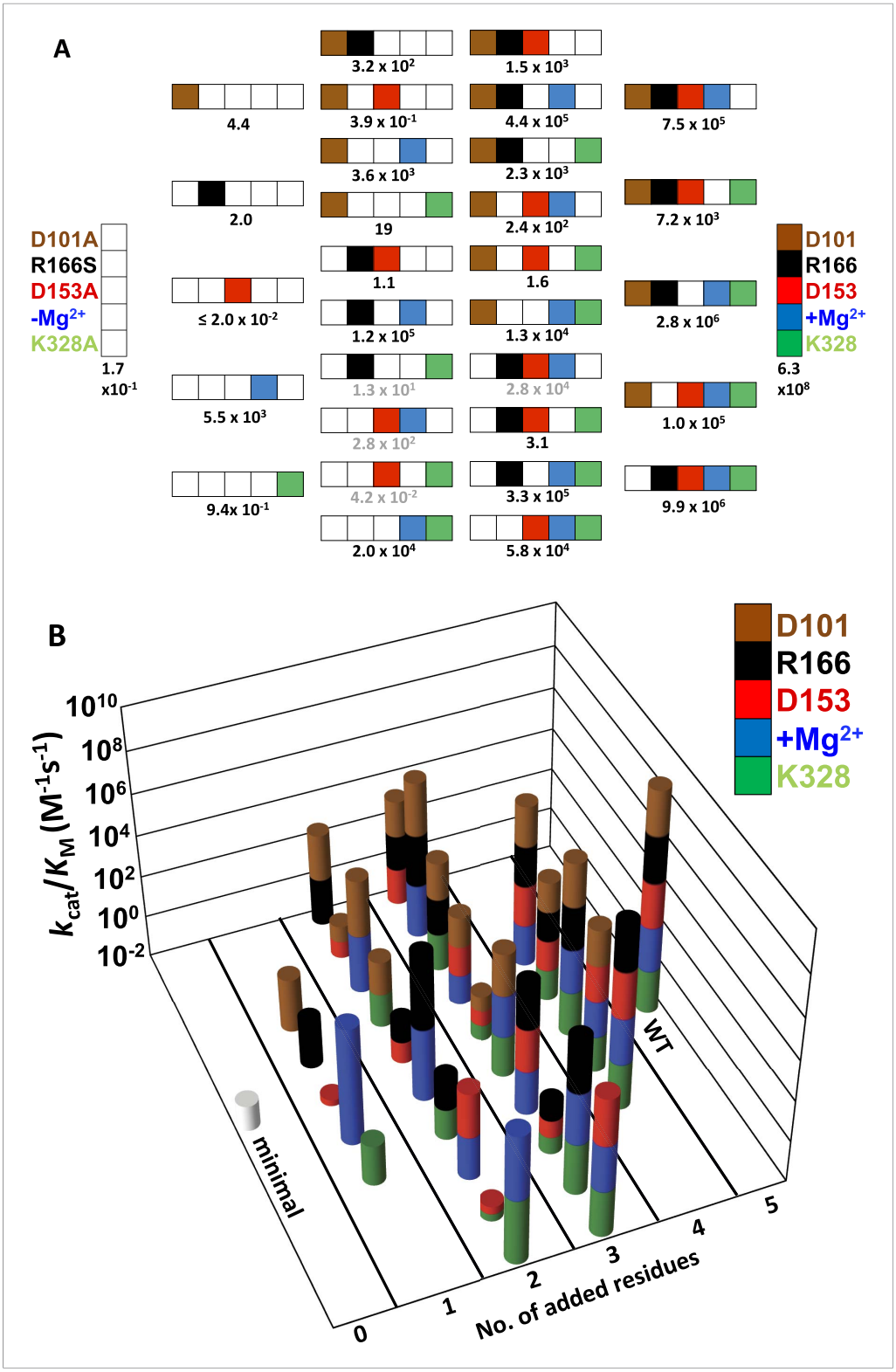

Figure 2. Catalytic efficiencies of AP variants for all combinations of five active site residues. (**A**) The 32 possible combinations of the five residues diagrammed with color-coding of residues as in ***Figure 1*** to represent whether a particular WT residue is present: D101, brown; R166, black; D153, red; K328, green; and E322 and the Mg^{2+} ion, blue; the absence of a WT residue at a particular position is indicated by a white square. The catalytic efficiency, k_{cat}/K_M ($M^{-1}s^{-1}$), of each combination is noted below each construct (***Table 1***). Rate constants calculated from the

Figure 2. continued on next page

Figure 2. Continued

energetic behavior of the functional units are shown in grey (***Table 1***). (**B**) Three-dimensional representation of the activities of the 32 AP variants, with the height of each bar corresponding to k_{cat}/K_M ($M^{-1}s^{-1}$ on a log scale) and the same color scheme as in (**A**).

DOI: 10.7554/eLife.06181.005

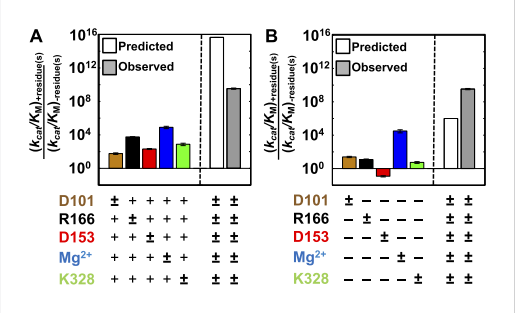

Figure 3. Single-mutation effects and additivity predictions. Rate effects from removing individual residues from WT AP (**A**) or restoring individual WT residues to AP minimal (**B**). The symbol (±) indicates which residue is varied. Residues are color-coded as in ***Figure 1***: D101, brown; R166, black; D153, red; K328, green; and E322 and Mg^{2+} ion, blue. The following mutations were made: D101A, R166S, D153A, K328A, and E322Y; several alternative mutations gave similar effects (***Appendix 1 Table 1***). To the right of the dashed line is the activity of WT AP relative to AP minimal observed (**A**, **B**, grey bars) and predicted from the effects of removal of each WT residue from the WT background and assuming independent (energetically additive) effects (**A**, open bar) or from the effects of addition of each WT residue in the minimal background, assuming independence (**B**, open bar).

DOI: 10.7554/eLife.06181.006

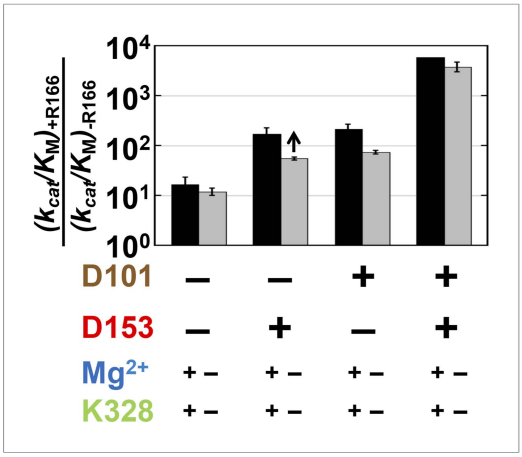

Figure 4. Catalytic effects of R166 in different mutant backgrounds. The effects of restoring R166 in different aspartate backgrounds with the Mg^{2+} ion and K328 present (black) or absent (grey). The arrow above the bar in the D153 background indicates that the ratio is a lower limit. Residues are color-coded as in ***Figure 1***, rate constants are from ***Table 1***, and mutations made are listed in ***Table 1***.

DOI: 10.7554/eLife.06181.007

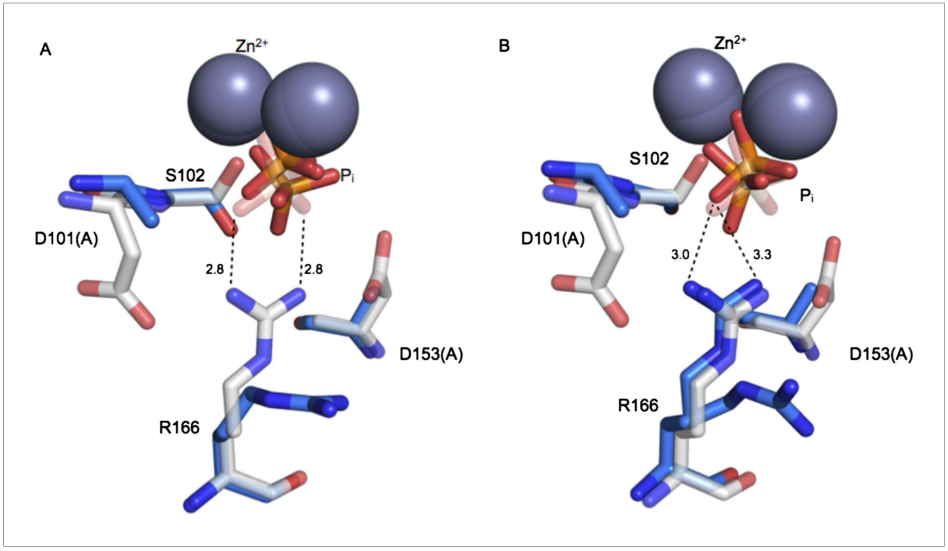

Figure 5. Structure of the active site of D101A/D153A AP. The active sites of the superimposed crystal structures of P_i-bound D101A/D153A AP (protein: blue, P_i: orange) and P_i-bound WT AP (protein: white, P_i: transparent). The two monomers of the AP dimer exhibit different active site configurations and are therefore both shown (**A**, **B**). (In contrast, the WT AP monomers are remarkably similar, as can be seen by comparing panels **A** and **B**.) In both monomers of D101A/D153A AP, P_i populates two positions that are distinct from its position in WT AP. (**A**) In one active site of D101A/D153A, R166 is rotated away from the active site. The hydrogen bond distances between R166 and P_i in WT AP are 2.8 Å (shown in **A**). (**B**) In the other active site of D101A/D153A, R166 partially occupies two positions, one of which faces the active site and hydrogen bonds to one of the partially occupied P_i ions. The other rotameric position adopted by R166 is flipped away from the active site, and presumably coincides with the other partially occupied P_i ion, as it would sterically clash with the active-site facing R166 rotamer. Hydrogen bond distances and angles for WT and D101A/D153A AP are listed in ***Appendix 2 Table 1***.

DOI: 10.7554/eLife.06181.009

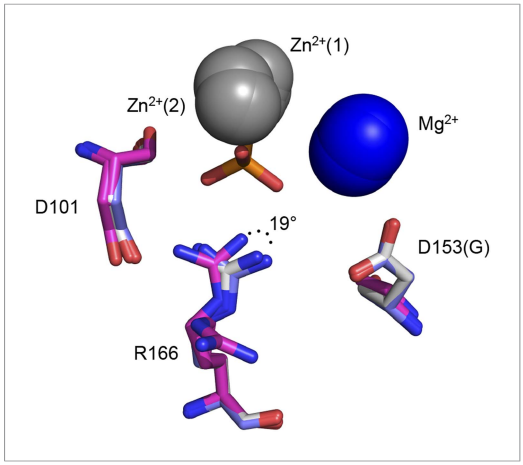

Figure 5—figure supplement 1. Ablation of D153 disrupts R166 positioning. Superimposed crystal structures of P_i-bound WT AP (purple, PDB 3TG0), apo WT AP (grey, PDB 1ED9), and apo D153G AP (magenta). In two independent structures of D153G AP, R166 is rotated from its position in P_i-bound WT AP by > 19˚ (PDB 1AJC) or rotated away from the active site (PDB 1AJD).

DOI: 10.7554/eLife.06181.010

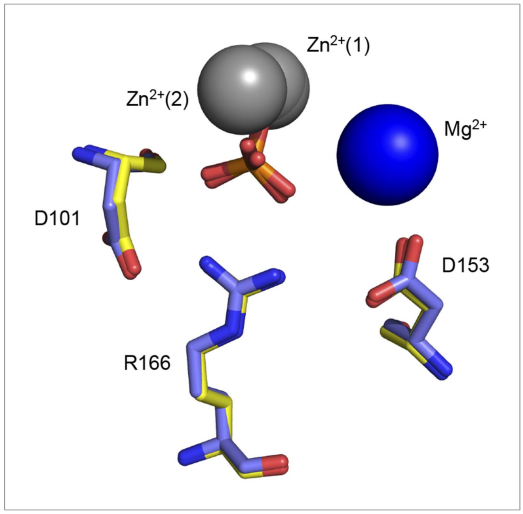

Figure 5—figure supplement 2. Removal of the active site Mg^{2+} ion does not disrupt R166 positioning. Superimposed crystal structures of P_i-bound E322Y AP (yellow, PDB 3DYC), which lacks the active site Mg^{2+} ion, and P_i-bound WT AP (purple, PDB 3TG0). R166 overlays closely in these structures.

DOI: 10.7554/eLife.06181.011

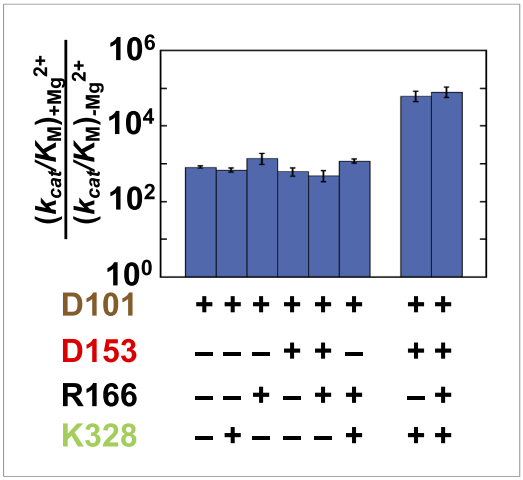

Figure 6. Catalytic effects of the Mg^{2+} ion in different mutant backgrounds. The effect of Mg^{2+} ion addition in different mutational backgrounds. Residues are color-coded as in ***Figure 1***, rate constants are from ***Table 1***, and mutations made are listed in ***Table 1***.

DOI: 10.7554/eLife.06181.012

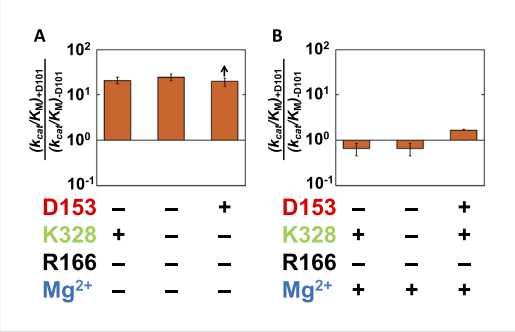

Figure 7. Catalytic effects of D101 in different mutant backgrounds. The effects of restoring D101 in backgrounds without bound Mg^{2+} (**A**) and with bound Mg^{2+} (**B**). The arrow indicates that the ratio is a lower limit. Residues are color-coded as in ***Figure 1***, rate constants are from ***Table 1***, and mutations made are listed in ***Table 1***. R166 is absent because it is also coupled with D101 (***Figure 4***).

DOI: 10.7554/eLife.06181.013

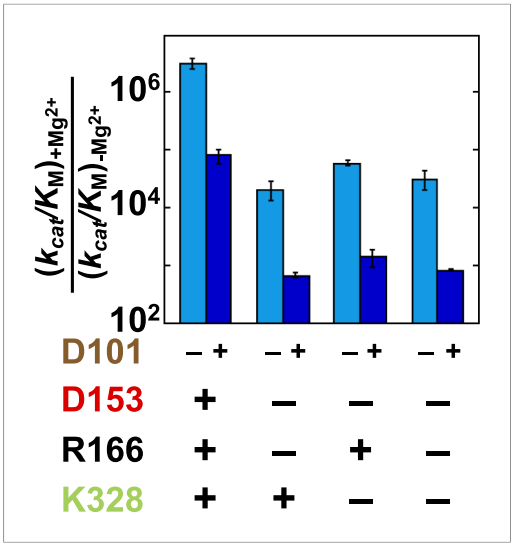

Figure 8. Catalytic effects of Mg^{2+} ion removal in mutant backgrounds without and with D101 present. The effects of restoring Mg^{2+} in the absence of D101 (light blue) and the presence of D101 (dark blue). Residues are color coded as in ***Figure 1***, rate constants are from ***Table 1***, and mutations made are listed in ***Table 1***.

DOI: 10.7554/eLife.06181.014

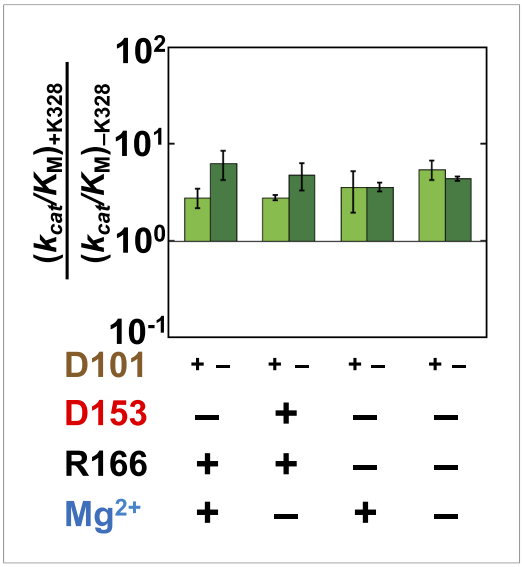

Figure 8—figure supplement 1. Effect of K328 addition with (light green) or without D101 (dark green) present. The effect of adding K328 is the same, within approximately twofold, whether D101 is present, indicating that these residues are essentially independent of one another.

DOI: 10.7554/eLife.06181.015

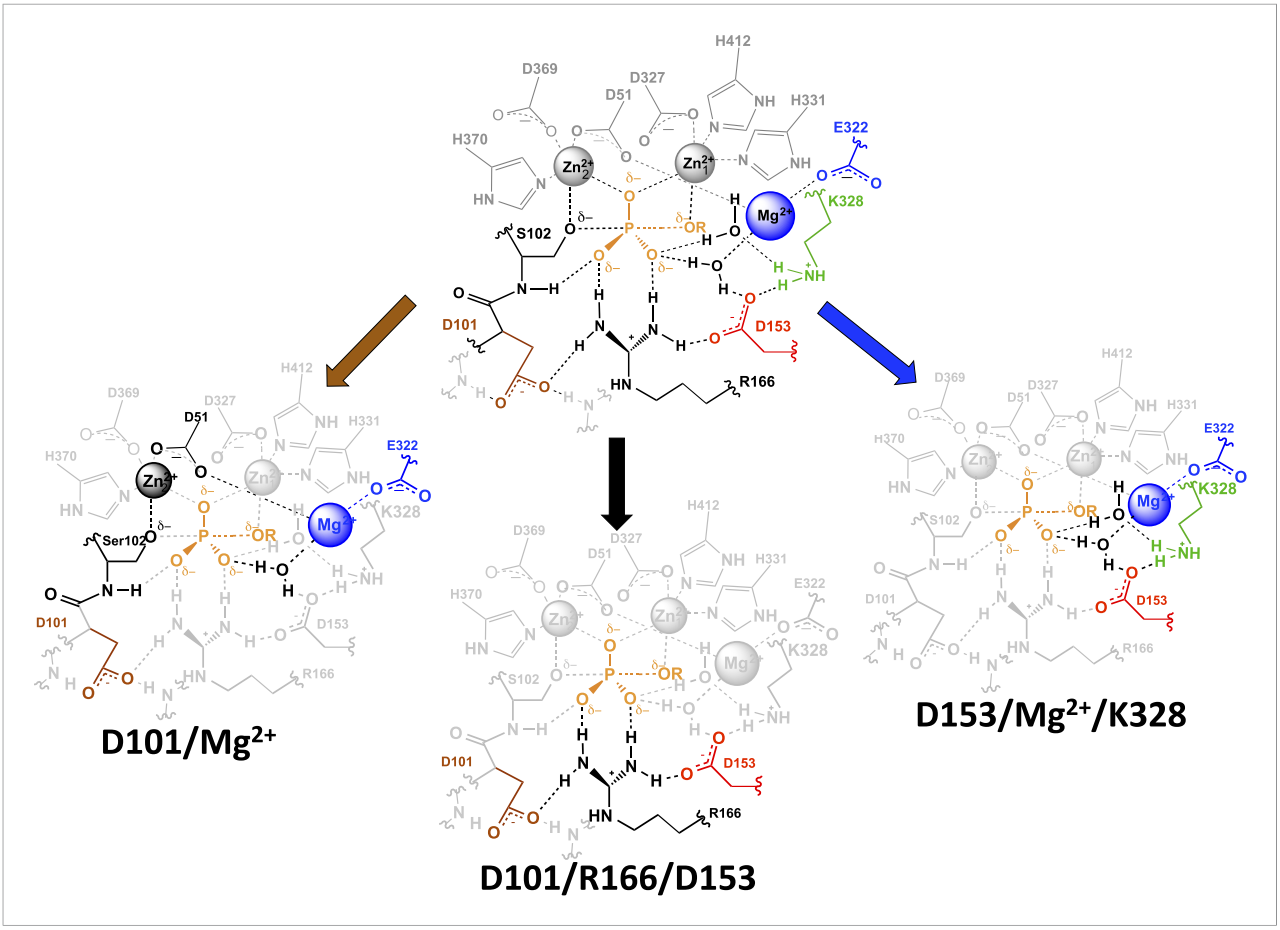

Figure 9. AP active site functional units. The residues of the functional unit are color-coded as in ***Figure 1***. For the D101/Mg^{2+} functional unit (left), the black residues and Zn^{2+} ion represent a potential route for the energetic connections between these residues.

DOI: 10.7554/eLife.06181.016

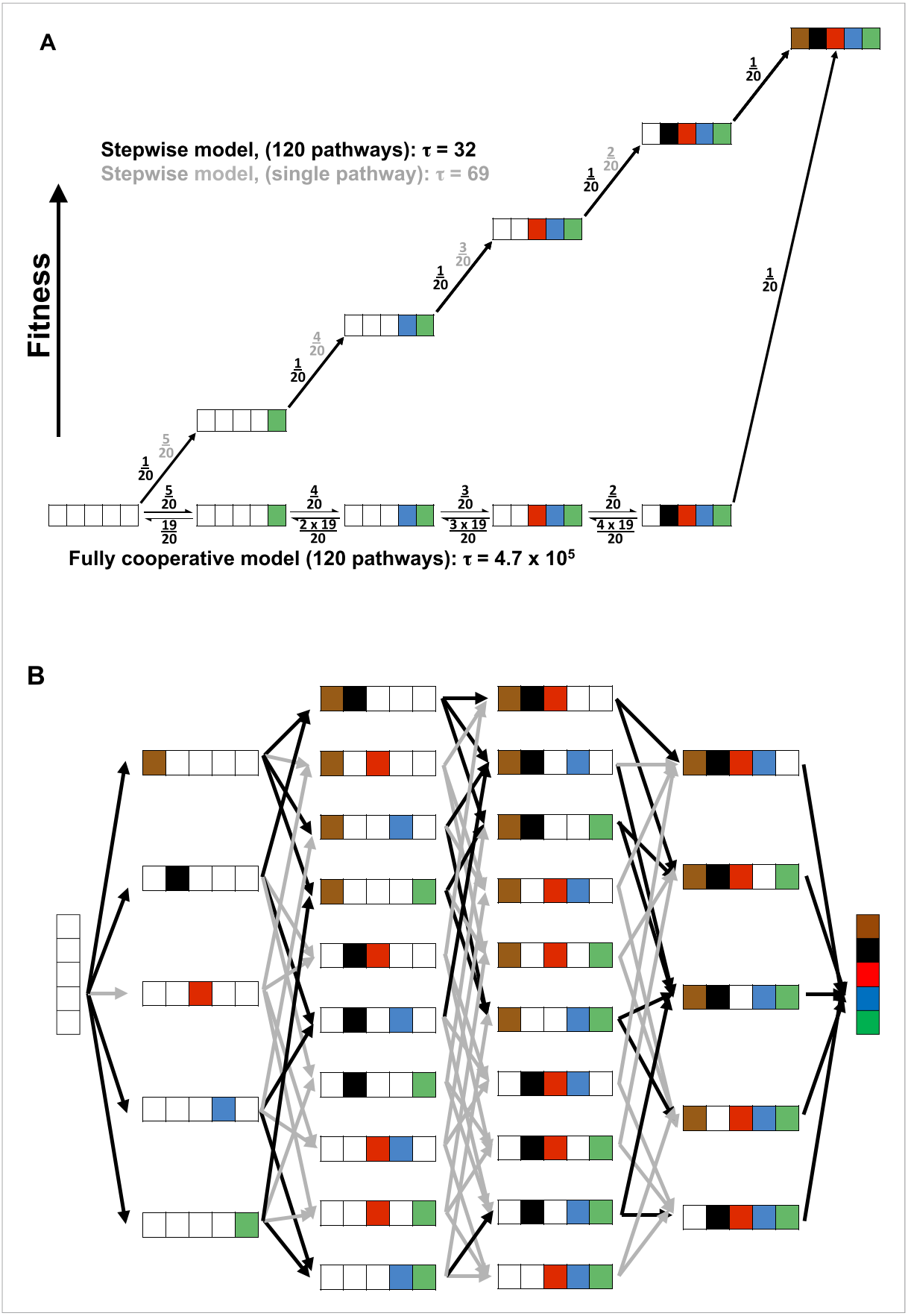

Figure 10. continued on next page

Figure 10. Continued

Figure 10. Cooperative and independent models of active site evolution. (**A**) Schematic comparing fully cooperative (bottom) and stepwise (top) models for a single pathway. In the fully cooperative model, simultaneous acquisition of all five WT residues is required to confer a selective advantage, leading to a mean waiting time of 4.7×10^5 (arbitrary units) considering all 120 pathways of adding in the residues (black net rates; for simplicity, only one intermediate of the multiple possible mutant combinations is shown in each step). In contrast, the stepwise model, in which acquisition of any WT residue confers a fitness advantage and is thus irreversible (top, black numbers), has a minimum mean waiting time of 32. If only one of the 120 pathways leads to a stepwise increase in fitness (top, grey numbers) then the mean waiting time would be 69. The model and simplifying assumptions made to highlight the differences arising from the presence or absence of cooperativity are described in Appendix 3. (**B**) Model of active site evolution showing the 120 possible paths in the AP landscape for introduction of the five residues investigated herein, in an otherwise WT background. A stepwise model in which acquisition of any WT residue is considered irreversible and all paths are possible would result in a mean waiting time of 32 (all arrows, grey and black, same as part **A**, top). As a subset of mutagenic steps toward WT AP (36 of the 80 potential evolutionary steps) confers a selective advantage (here defined as a rate increase of >threefold) and paths containing steps that do not confer such an advantage have much lower probabilities, we consider the 34 of 120 pathways that provide a monotonic fitness increase as all five WT residues are added. This gives a mean waiting time between the mean waiting times for the stepwise models for a single pathway and 120 pathways, 32 and 69, respectively.

DOI: 10.7554/eLife.06181.017